Interaction effects in a one-dimensional constriction

K. J. Thomas, J. T. Nicholls, N. J. Appleyard, M. Y.Simmons, M. Pepper, D. R. Mace, W. R. Tribe, and D. A. Ritchie
Cavendish Laboratory, Madingley Road, Cambridge CB3 0HE, United Kingdom
(Received 1 December 1997; revised manuscript received 20 April 1998)

We have investigated the transport properties of one-dimensional (1D) constrictions defined by split-gates in high quality GaAs/$Al_xGa_{1-x}As$ heterostructures. In addition to the usual quantized conductance plateaus, the equilibrium conductance shows a structure close to $0.7(2e^2/h)$, and in consolidating our previous work [K. J. Thomas *et al.*, Phys. Rev. Lett. **77**, 135 (1996)] this *0.7 structure* has been investigated in a wide range of samples as a function of temperature, carrier density, in-plane magnetic field $B_\parallel$, and source-drain voltage V_{sd}. We show that the 0.7 structure is not due to transmission or resonance effects, nor does it arise from the asymmetry of the heterojunction in the growth direction. All the 1D subbands show Zeeman splitting at high $B_\parallel$, and in the wide channel limit the g factor is $|g|\approx 0.4$, close to that of bulk GaAs. As the channel is progressively narrowed we measure an exchange-enhanced g factor. The measurements establish that the 0.7 structure is related to spin, and that electron-electron interactions become important for the last few conducting 1D subbands. [S0163-1829(98)05032-2]

I. INTRODUCTION

When a negative gate voltage is applied to a lithographically defined split-gate, the underlying two-dimensional electron gas (2DEG) is electrostatically squeezed into a one-dimensional (1D) channel.[1] In a clean 1D constriction, where the mean free path is much longer than the effective channel length, the conductance is quantized[2,3] in units of $2e^2/h$; a result that can be understood as the adiabatic transmission of 1D subbands. In an earlier paper[4] we showed that, in addition to the usual quantized conductance plateaus, there is also a structure at $0.7(2e^2/h)$. This so-called *0.7 structure* shows characteristics that demonstrate the importance of many-body interactions in the limit of a few conducting 1D subbands.

As a consequence of electron-electron interactions, a 1D electron gas is expected to exhibit Tomonaga-Luttinger[5,6] (TL) liquid behavior rather than Fermi liquid behavior. In addition to a TL liquid there are other possible states of an interacting 1D system, for example, a 1D Wigner crystal is predicted[7] when the 1D electron density is less than the $(\text{Bohr radius})^{-1}$. It has also been shown[8] that at sufficiently low electron densities the exchange interactions will dominate over the kinetic energy, and a three-dimensional electron gas will undergo a transition to a ferromagnetic state. The increasing importance of the exchange interactions in lower dimensions is borne out by recent calculations[9,10] that show a similar spontaneous spin polarization in a quasi-one-dimensional electron gas.

In light of these ideas we present experimental evidence showing that electron-electron interactions are important in a ballistic 1D constriction. We do not observe TL liquid behavior, but we believe there is evidence for spontaneous spin polarization. We expand upon our earlier work,[4] showing results for six different samples. The rest of this paper is organized as follows. Section II gives a brief review of split-gate devices, and a description of the samples and measurements is provided in Sec. III. The zero-field gate characteristics as a function of temperature and 2D carrier density are presented in Sec. IV A, and measurements in a strong in-plane magnetic field and with an applied source-drain voltage in Secs. IV B and IV C, respectively. We discuss our results, and their relevance to the TL model in Sec. V.

II. REVIEW OF SPLIT-GATE DEVICES

Split-gates[1] are a well established[11] technique for creating a smooth one-dimensional constriction in a 2DEG. When a negative voltage V_g is applied to a lithographically defined pair of Schottky split-gates above a GaAs/$Al_xGa_{1-x}As$ heterostructure, shown in Fig. 1(a), the 2DEG is depleted from beneath the gates and a 1D channel is left defined between them. If the elastic mean free path l_e is much greater than the width W and length L of the channel, transport through the 1D constriction is ballistic and the differential

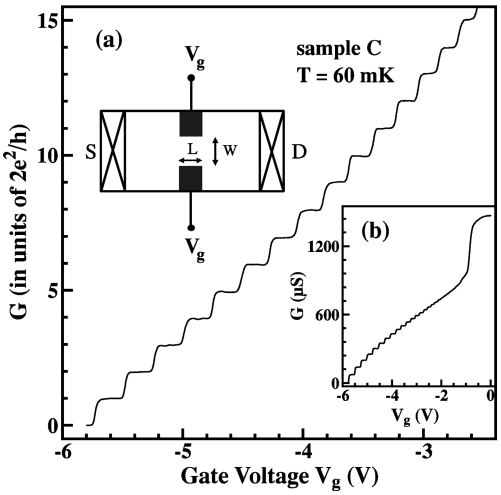

FIG. 1. The differential conductance $G(V_g)$ of sample C at $T=60$ mK, after correction for a series resistance of $R_S=703\Omega$. Insets: (a) Schematic of a split-gate device, where S and D represent the source and drain contacts. (b) Raw data showing the definition and pinch-off characteristics.

TABLE I. Sample properties.

Sample[a]	Structure[b]	2DEG depth (μm)	Mobility[c] μ (10^6 cm^2/Vs)	Carrier density n_{2D} (10^{11} cm^{-2})	Split-gate[d] width W (μm)
A	SH	0.28	4.5	1.8	0.75
B	SH	0.31	3.5	1.4	0.95
C	SH	0.28	4.5	1.8	0.95
D	SH	0.31	3.5	1.4	0.75
E	SH	0.29	3.5	1.3	0.75
F	QW	0.17	4.8	2.4	0.75

[a]Samples A and B were used in Ref. 4.
[b]SH=single heterojunction, QW=quantum well of width 200 Å.
[c]The low temperature mobility μ and carrier density n_{2D} were measured at zero back gate voltage after illumination with a red light-emitting diode.
[d]All split-gates have a length $L=0.4$ μm.

conductance, $G(V_g)=N(2e^2/h)$, is quantized,[2,3] where N is the number of transmitted 1D subbands. At small negative gate voltages, when a wide 1D channel is first defined, the lateral confinement potential is best described by a square well with a width similar to the lithographic separation W of the split-gates, and an electron density equal to that of the bulk 2DEG (n_{2D}). The carrier density and width of the channel are progressively reduced as V_g becomes more negative, and when there are only two or three occupied 1D subbands the electrostatic landscape around the narrowest part of the constriction can be modeled by a saddle-point potential.[12] Split-gate structures have been used to study electron focussing,[13] nonlinear transport,[14,15] and magnetic depopulation,[16] all of which can be interpreted in a noninteracting electron picture. Recent conductance measurements[4] of clean split-gate devices exhibit a structure at $0.7(2e^2/h)$ that cannot be explained within a noninteracting picture.

In this paper, as well as in recent work,[4,17] the 1D constrictions are defined in deep heterostructures where the 2DEG is up to 3000 Å below the sample surface. Using these high purity 2DEGs (with a low temperature mobility as high as 4.8×10^6 cm^2/Vs) we have measured more than 20 ballistic conductance plateaus, with a high degree of flatness that reflects the lack of potential fluctuations in the constriction. The samples show well-defined 1D characteristics with little intersubband scattering, even between the closely spaced (0.5 meV) higher subbands. With a magnetic field applied in the plane of the 2DEG, each doubly degenerate 1D subband is split by a Zeeman energy. Spectroscopy of the 1D subbands can be performed[14] using a dc source-drain voltage V_{sd} and we have used this to measure the g-factors of the 1D subbands.[18]

III. SAMPLES AND EXPERIMENTAL DETAILS

A. Device fabrication

Measurements are presented here for six samples, fabricated from 2DEGs formed in modulation-doped GaAs/$Al_{0.33}Ga_{0.67}$As heterostructures, grown by molecular beam epitaxy (MBE) on a (100) semi-insulating GaAs substrate. The sample properties are listed in Table I.

For the single heterojunction samples (A–E), the 2DEG is formed at the interface between a thick (1–2 μm) undoped GaAs buffer layer and a 600–1000 Å undoped $Al_xGa_{1-x}As$ spacer layer. Doping is provided by 2000 Å of Si-doped $Al_xGa_{1-x}As$ (1.2×10^{17} cm^{-3}), which is capped with 170 Å of undoped GaAs. The use of lightly doped $Al_xGa_{1-x}As$ and a thick spacer layer reduces the remote ionized impurity scattering and enhances the mobility. The growth sequence for the quantum well sample (F) starts with a 100-period 25 Å GaAs/$Al_xGa_{1-x}As$ superlattice buffer, which is used to trap surface impurities from the substrate, and to progressively improve the interface smoothness. This is followed by 1000 Å of $Al_xGa_{1-x}As$ ramped from $x=0$ to $x=0.33$, and a 0.45 μm buffer with $x=0.33$. Below the 200 Å GaAs quantum well there is a 2000 Å Si-doped $Al_{0.33}Ga_{0.67}As$ (1.2×10^{17} cm^{-3}) layer and an 800 Å $Al_xGa_{1-x}As$ spacer, and above there is a 1000 Å spacer and a 400 Å doped ($Al_{0;33}Ga_{0.67}As$ (1×10^{18} cm^{-3}) layer. The wafer is capped with 170 Å of undoped GaAs. On the back of all the wafers there is indium used to mount the samples during MBE growth; this diffuses approximately 150 Å into the GaAs substrate, and forms a back gate 350 μm below the 2DEG. When the back gate voltage V_{bg} is changed from -100 V to $+50$ V, there is a 30% increase of the carrier density n_{2D}.

The samples were first patterned into Hall bars. Ohmic contacts were made by thermal evaporation of Au/Ge/Ni alloys, which were annealed for 80 seconds at 430 °C in a N_2/H_2 atmosphere. Split-gates were then patterned by electron-beam lithography followed by thermal evaporation of 15 nm NiCr and 35 nm Au. All the split-gates had a length $L=0.4$ μm, with widths W given in Table I.

B. Experimental details

The two-terminal differential conductance of the samples, $G=dI/dV$, was measured at low temperatures (0.05–4 K) in a dilution refrigerator using a constant excitation voltage of 10 μV at 85 Hz. Measurements were also performed with a high in-plane magnetic field ($B_\parallel$) applied parallel to the current through the 1D constriction. To check for an out-of-plane field component due to misalignment, we monitored the Hall voltage; from such measurements we were able to align samples to better than 1°.

We use a technique developed by Patel *et al.*[18] to deduce the energy separation of 1D subbands from the effects of an applied dc source-drain voltage V_{sd}. A peak occurs in the

transconductance dG/dV_g (obtained by numerical differentiation of the conductance) at the gate voltage where there is a step in $G(V_g)$. There is a crossing of adjacent transconductance peaks when $eV_{sd}=\Delta E_{N,N+1}$, where $\Delta E_{N,N+1}$ is the energy separation between the N and $N+1$ subbands.[18] A doubling of the transconductance peaks can also be brought about using a strong in-plane magnetic field to lift the spin degeneracy of the 1D subbands. The g-factor can be determined by comparing the voltage V_{sd} required to produce the same amount of splitting as the magnetic field, and comparing the two energy scales[14]

$$eV_{sd}=2g_{\|}\mu_B B_{\|}S. \tag{1}$$

This technique is valid if the transconductance peak splittings are linear in both $B_{\|}$ and V_{sd}.

All conductance characteristics have been corrected for a series resistance (R_S) that is typically less than 2 kΩ; this includes contributions from the 2DEG, the contact resistances between the Ohmic contacts and the 2DEG, and the wires down the probe. Series resistance corrections have also been applied to the source-drain measurements.

IV. RESULTS

A. Zero-field conductance characteristics

Figure 1 shows the gate characteristics $G(V_g)$ of sample C at 60 mK. As the gate voltage V_g is made negative the 2DEG beneath the split-gates is depleted at $V_g=-0.9$ V, giving a sharp drop in the conductance shown in the overall characteristics in Fig. 1(b). Once the 1D channel is defined, further decreases of V_g narrow the channel and reduce the carrier density in the vicinity of the constriction; as a result the 1D subbands are depopulated and the conductance decreases in steps of $2e^2/h$. The constriction pinches off at $V_g=-5.75$ V, when all the 1D subbands are depopulated. Overall, there are 25 well-resolved conductance plateaus; the last 15 are shown in the main figure, after correction for a series resistance of $R_S=703\ \Omega$. The plateaus are quantized at $N(2e^2/h)$ to within 1% accuracy.

In addition to the usual quantized conductance plateaus, there is a structure at $0.7(2e^2/h)$, seen in all samples. This is shown in Fig. 2 for two devices, one based on a quantum well (sample F), and the other on a standard heterojunction (sample D) measured at $T=1.5$ K. The 0.7 structure is not as precisely quantized as the conductance plateau at $2e^2/h$, but is observed in the range $0.65-0.75(2e^2/h)$.

The 0.7 structure has distinctive dependences on carrier density and temperature. Figure 3(a) shows the gate characteristics $G(V_g)$ of sample E for different 2D carrier densities. As n_{2D} is decreased from 1.4 to 1.1×10^{11} cm^{-2} using the back gate, the pinch-off voltage becomes more positive. At the highest density, shown in the left hand trace, the 0.7 structure is visible only as a weak knee in the gate characteristics, which develops into a stronger structure as n_{2D} is reduced. Figure 3(b) shows the conductance $G(V_g)$ at $n_{2D}=1.3\times10^{11}$ cm^{-2} as the temperature is raised from 0.1 to 1.2 K in steps of 0.1 K. The pinch-off voltage remains independent of temperature. The plateau at $2e^2/h$ becomes thermally smeared at the highest temperature, whereas the 0.7 structure becomes stronger, in agreement with previous

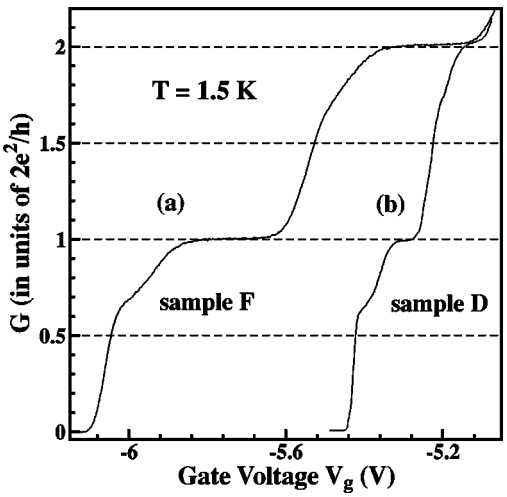

FIG. 2. Conductance characteristics of 1D constrictions defined in (a) a quantum well, and (b) a conventional heterostructure.

measurements[4] of sample B. Figure 3(c) shows the temperature dependence at $n_{2D}=1.0\times10^{11}$ cm^{-2}; at this lower electron density the more prominent 0.7 structure is less sensitive to temperature. At higher temperatures, $T\sim10$ K, the 0.7 structure disappears; we tentatively ascribe to the structure a characteristic energy of order 1 meV.

By applying different voltages to the two arms of the split-gate the 1D channel can be moved laterally,[19,20] allowing the electrostatic potential landscape between the split-gates to be scanned. Figure 4 shows the conductance characteristics obtained when the two arms of the split-gate are swept together, but maintaining a constant voltage difference ΔV_g between them. A change of ΔV_g from 0 to 1.3 V moves the channel by 80 nm; the plateau at $2e^2/h$ is unaffected by the shift (as are the higher index plateaus) showing that the constriction is free of impurities. In this sample the 0.7 structure occurs at $0.65(2e^2/h)$, and is also unchanged by the lateral shift of the channel.

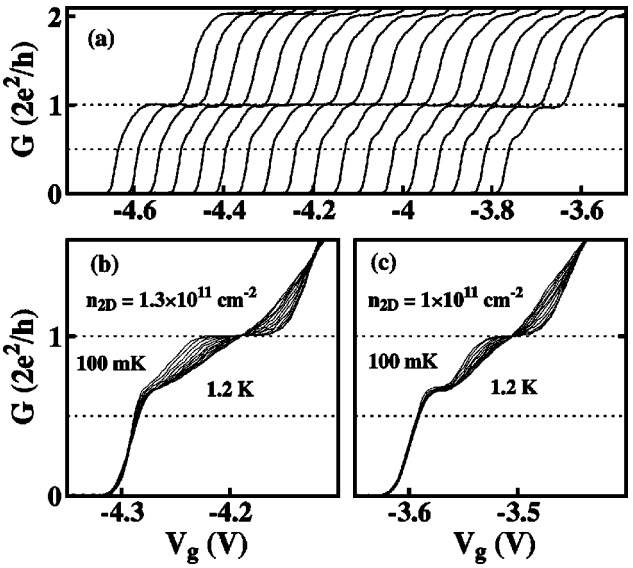

FIG. 3. (a) The 0.7 structure in sample E at 60 mK going from left to right n_{2D} is reduced from 1.4×10^{11} cm^{-2} ($V_{bg}=60$ V) to 1.1×10^{11} cm^{-2} ($V_{bg}=-110$ V) in steps of 1.8×10^{9} cm^{-2}. The temperature dependence of the 0.7 structure, in steps of 0.1 K, at (b) $n_{2D}=1.3\times10^{11}$ cm^{-2} and (c) 1.0×10^{11} cm^{-2}.

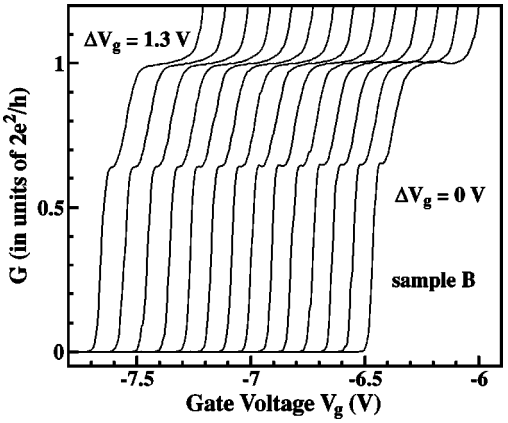

FIG. 4. Lateral shifting of the channel in sample B at $T=60$ mK, using an offset voltage ΔV_g between the two arms of the split-gate. Each time ΔV_g is incremented by 0.1 V, the center of the 1D channel is shifted by 6.2 nm.

B. Magnetic field dependence

A strong in-plane magnetic field $B_\parallel$ lifts the spin degeneracy of the 1D subbands giving conductance plateaus quantized in units of e^2/h. Figure 5 shows how the transconductance peaks in sample D split as $B_\parallel$ is increased in steps of 1 T. As previously observed[4] in sample A, there is an overall parabolic shift of the gate characteristics with $B_\parallel$ that can be attributed to a diamagnetic shift of both the 1D and 2D subband edges.[21] Satellite peaks, marked with an asterisk (*) and a solid bullet (●), corresponding to the conductance structures at $0.7(2e^2/h)$ and $1.7(2e^2/h)$, grow out of the right hand shoulders of the zero-field transconductance peaks. At the highest magnetic field, $B_\parallel=16$ T, the transconductance peaks have roughly equal integrated areas, with the zeros between them corresponding to the conductance plateaus quantized in units of e^2/h. The Fig. 5 inset shows the

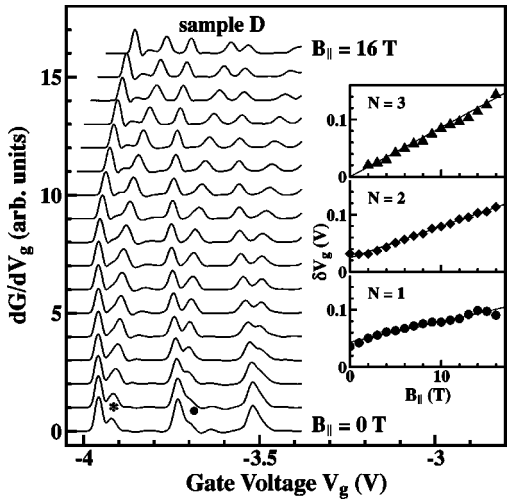

FIG. 5. The transconductance dG/dV_g of the first three subbands of sample D as $B_\parallel$ is incremented in steps of 1 T. The peaks indicated with an asterisk (*) and a solid bullet (●) show the conductance features at $0.7(2e^2/h)$ and $1.7(2e^2/h)$ at $B_\parallel=0$ T. The inset shows the magnetic field induced gate voltage splittings, $\delta V_g(B_\parallel)$, for subband indices $N=1$, 2, and 3. The solid lines are least-squares linear fits to the data.

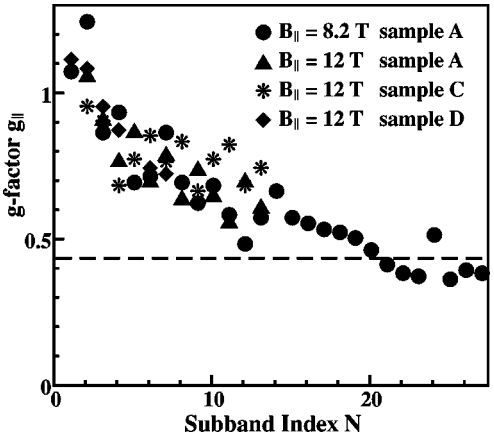

FIG. 6. The in-plane g factor $g_\parallel$ as a function of subband index N. The dashed line at $|g|=0.44$ indicates the g factor for bulk GaAs.

voltage splitting $\delta V_g(B_\parallel)$ for the first three subbands. The Zeeman splittings are linear in $B_\parallel$, and at zero field the peak separation $\delta V_g(0)$ is finite for both $N=1$ and 2; this demonstrates that the zero-field 0.7 structures evolve continuously into spin-split half-plateaus as the magnetic field is increased. By comparing $\delta V_g(0)$ to a V_{sd}-induced splitting, we estimate the zero-field energy gap as $\Delta_1=1.1$ meV for the lowest subband, and $\Delta_2=0.43$ meV for $N=2$. In our previous measurements[4] of sample A we measured a zero-field gap $\Delta_1=1$ meV. In measurements of samples A and D the energy Δ_1 is comparable to the temperature at which the 0.7 structure smears out.

From the splitting of the transconductance peaks in $B_\parallel$ and V_{sd}, Eq. (1) is used to determine the g factors for all 1D subbands.[22] Figure 6 shows $g_\parallel$ measured as a function of subband index N for three different samples, as well as showing results for sample A at two different magnetic fields. When the channel is wide and there are many 1D subbands, the measured $g_\parallel$ is close to the bulk GaAs value[23] $|g|\approx 0.4$. As the number of occupied 1D subbands decreases there is an enhancement of $g_\parallel$.

C. The effect of a source-drain voltage V_{sd}

The effect of a source-drain voltage V_{sd} on the conductance characteristics $G(V_g)$ has been studied in detail in Ref. 14. As V_{sd} is increased, half-plateaus appear at $(N+\frac{1}{2})2e^2/h$ for $G>2e^2/h$, whereas V_{sd}-induced structures appear at $0.85(2e^2/h)$ and $0.3(2e^2/h)$ for $G<2e^2/h$. The gate voltage scale is a smooth measure of the 1D confinement energy, so a greyscale plot of the transconductance (similar to those presented in Ref. 17) allows us to follow the energy shifts of subband features. Figure 7(a) shows how the gate voltage positions of transconductance features for the lowest three subbands move as a function of V_{sd} at $T=1.4$ K. The dark lines show transitions between plateaus and the white regions are the conductance plateaus (where the numbers denote the conductance in units of $2e^2/h$). Features moving to the right (left) with increasing V_{sd} do so as the electrochemical potential of the source (drain) crosses a subband edge, and if the subband energies were independent of their occupation we would expect a linear evolution of the

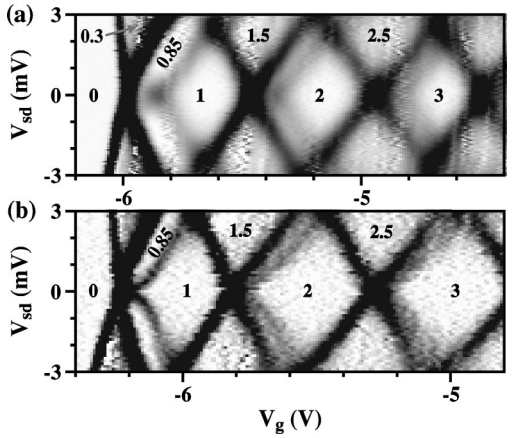

FIG. 7. Greyscale plots of the zero-field transconductance of sample F as a function of V_{sd} at (a) $T=1.2$ K, and (b) $T=50$ mK. The numbers indicate the plateau conductances in units of $2e^2/h$, and the 0.7 structure is the bright region at $V_{sd}=0$ between $G=0$ and $G=2e^2/h$ in the higher temperature data. The usual linear splitting does not occur for features associated with the 0.7 structure, indicating that the energies of these features are sensitive to the occupation of the subband. Note that similar features are seen for $N=2$ and $N=3$. The data in (a) and (b) were measured a week apart, over which time there was a slight change in the gate voltage characteristics of the device.

transconductance structures with V_{sd}. This is clearly not the case for the features associated with the 0.7 structure in the lowest subband, suggesting that the subband configuration is occupation-dependent, for which an interaction effect could be responsible. In Fig. 7(b), we present data taken at $T=50$ mK, when the 0.7 structure is no longer visible at $V_{sd}=0$. As the electrochemical potential in the drain is lowered below that of the source, a feature separates from the $N=1$ subband edge, giving rise to a white region that corresponds to a plateau at $0.85(2e^2/h)$.[14] Similar structures with smaller separations can be seen in Fig. 7(b) for $N=2$ and $N=3$.

V. DISCUSSION

A. Evidence for a spin mechanism

In all the 18 samples from seven different wafers that we have studied, the 0.7 structure is observed on all cool-downs. The structure has been measured in both pointed[24] and rectangular split-gates, in single heterojunction samples and in quantum wells, and is independent of the distance of the 1D electron gas from the confining gate.[4,14] Recently, Kristensen *et al.*[25] have observed a clear 0.7 structure in wires fabricated by shallow etching, which provide stronger electrostatic confinement than conventional split-gate structures. Some evidence of additional structure has also been reported for GaAs wires[26] patterned by focussed ion beam and InP based quantum wires,[27] though in both cases the samples are not of high mobility. We believe that the 0.7 structure is an intrinsic property of clean 1D ballistic constrictions at low electron densities.

Additional structures in the gate characteristics of a ballistic 1D constriction could be caused by impurity effects.[28] Close to pinch-off the carrier density around the constriction may become inhomogeneous,[29] and the charging characteristics of small puddles of electrons can give rise to Coulomb blockade peaks in the $G(V_g)$ characteristics.[30] Transmission resonances due to the multiple reflection of electrons can also introduce conductance features below $2e^2/h$. Our measurements cannot be explained by either of these mechanisms, as both Coulomb blockade peaks and resonance phenomena undergo an energy averaging at finite temperature that smears out their structure, whereas Fig. 3 shows the 0.7 structure becoming stronger when the temperature is initially raised. It is also common that impurity effects differ between sample cool-downs, which we do not observe. The clean quantized conductance plateaus (see Fig. 1) and the absence of additional structures when the channel is moved from side to side (Fig. 4) demonstrate the lack of potential fluctuations in and around the 1D constriction in our samples.

If the 0.7 structure were a transmission effect, unrelated to spin, it would be replicated at $0.35(e^2/h)$ when the spin degeneracy was lifted by an applied magnetic field. This is not observed in the high-field measurements shown in Fig. 5, suggesting that the zero-field intercepts of the spin splitting are related to a spontaneous lifting of the spin degeneracy in the lowest subbands. A spontaneous spin polarization driven by an exchange interaction is predicted in a dilute 1D electron gas for both hard-wall cylindrical[31] and parabolic[9,10] confinements, and the enhancement of the in-plane g-factor shown in Fig. 6 underlines the importance of exchange effects as the 1D subbands are depopulated.[4,18,32] Figure 3(a) shows that the 0.7 structure strengthens as n_{2D} is lowered, behavior that is consistent with an exchange interaction mechanism. Further evidence that an exchange mechanism may be responsible for the 0.7 structure is provided by the source-drain measurements in Fig. 7, where the features in the lowest subband are sensitive to the occupation statistics in the channel.

Zero-field spin splitting could also arise from the spin-orbit interaction, either from the inversion asymmetry of the conduction band of GaAs, or internal electric fields due to the asymmetry of the confinement in the growth direction. However, the energy of the spin-orbit term due to the inversion asymmetry is calculated[33] to be only $\sim 10^{-2}$ K, and measurements of the quantum well sample (see Fig. 2) show that the 0.7 structure is not weakened when the confinement is less asymmetric.

Another mechanism for a spin polarization is based[34] on the assumption that electron-electron scattering rates for hot electrons in a 1D channel will be different for spin-up and spin-down electrons. However, the 0.7 structure is observed in equilibrium measurements ($V_{sd}=0$) when there are no hot electrons.

In summary, the 0.7 structure appears to be linked to spontaneous lifting of spin degeneracy in the 1D constriction, driven by an electron-electron interaction effect, and the evidence is initially consistent with this being the exchange interaction. A spontaneous spin polarization of the electron gas, however, is expected to give rise to a conductance plateau at $0.5(2e^2/h)$, rather than a structure at $0.7(2e^2/h)$. To address this point Wang and Berggren[35] propose that if the height of the saddle-point potential is different for the two different spin orientations, then propagation of one spin-split subband with some tunneling transmission probability for the other spin may give a conductance above $0.5(2e^2/h)$. In an

alternative theory, Schmeltzer *et al.*[36] propose that within TL theory there is a hybridization of the up and down spins in the last subband.

The temperature dependence of the 0.7 structure, where initially the feature becomes stronger with increasing temperature, is also surprising; a straightforward spin polarization is expected to weaken with increasing temperature. There is instead a characteristic temperature (1.5 K) at which the 0.7 structure is most prominent, and measurements[25] of the activated behavior of the 0.7 structure support this view.

B. Relevance to the TL model

As a consequence of electron-electron interactions, a 1D electron gas is expected to exhibit Tomonaga-Luttinger[5,6] liquid behavior. It is predicted[37] that the conductance of a clean one-dimensional wire with a single conducting mode may be renormalized to a value $K(2e^2/h)$, where $K>1$ for attractive interactions, and $K<1$ for repulsive interactions. It was later argued[38–40] that such a conductance renormalization may not occur, because the measured contact resistance is determined by noninteracting electrons that are injected from the contacts into the 1D wire. Impurity scattering, however, may give rise to corrections to the low temperature dc conductance due to temperature and the finite length of the system.[41,42]

TL liquid behavior has been investigated in quantum wires fabricated by two different techniques. Tarucha *et al.*[43] fabricated 2–10 μm long 1D wires using wet etching and gating, and although no renormalization of the conductance quantization was observed, the temperature dependence of the last plateau is consistent with an interaction parameter $K\approx 0.7$ when fitted to a modified TL theory.[41] Using cleaved edge overgrowth, Yacoby *et al.*[44] have fabricated wires of length 1–20 μm that are strongly confined in both directions perpendicular to the wire axis. The wires have extremely high L/W ratios, and clean conductance plateaus were observed, but quantized in units of $\alpha(2e^2/h)$, where $0.75<\alpha \leqslant 1$ and were both sample and temperature dependent. Recent theoretical work[45] shows that these experimental results may be a consequence of enhanced backscattering at the interface between the 1D wire and the connecting 2DEG regions, and that the nonuniversal quantization is not an intrinsic property of a one-dimensional electron gas. There is stronger evidence for TL behavior in the fractional quantum Hall regime.[46,47]

We emphasize that our results are different from Yacoby *et al.*,[44] in that we observe a plateau at $2e^2/h$ *and* a structure at $0.7(2e^2/h)$, whereas they observe nonuniversal quantization of the integer plateaus. Though our results are not inconsistent with the TL as opposed to the Fermi liquid description of the system, the effects that we present here are of a different type, and relate to interactions between the two one-dimensional liquids in opposite spin states. A model that includes spin-spin interactions will therefore be necessary to adequately model our results.

VI. CONCLUSIONS

In all the samples investigated, we observe clean quantized conductance plateaus as well as the structure at $0.7(2e^2/h)$. We have shown that the 0.7 structure is not due to transmission or resonance effects, nor does it arise from the asymmetry of the heterojunction in the growth direction. The structure is not precisely quantized at $0.7(2e^2/h)$, and in a strong in-plane magnetic field it moves to $0.5(2e^2/h)$. The origin of this 0.7 structure cannot be described by either the Tomonaga-Luttinger theory or a simple spin polarization of the electron gas, but we believe the exchange-enhanced g factor and the nonlinear behavior of subband features with an applied voltage to provide strong evidence that interaction effects are becoming increasingly important as the 1D channel depopulates, and that the origin of the 0.7 structure is related to spin.

ACKNOWLEDGMENTS

We thank the Engineering and Physical Sciences Research Council (U.K.) for supporting this work. K.J.T. acknowledges support from the Association of Commonwealth Universities, and D.A.R. acknowledges support from Toshiba Cambridge Research Center. We thank Dr. A.V. Khaetskii and Dr. C.H.W. Barnes for useful discussions.

[1] T. J. Thornton, M. Pepper, H. Ahmed, D. Andrews, and G. J. Davies, Phys. Rev. Lett. **56**, 1198 (1986).

[2] D. A. Wharam, T. J. Thornton, R. Newbury, M. Pepper, H. Ahmed, J. E. F. Frost, D. G. Hasko, D. C. Peacock, D. A. Ritchie, and G. A. C. Jones, J. Phys. C **21**, L209 (1988).

[3] B. J. van Wees, H. van Houten, C. W. J. Beenakker, J. G. Williamson, L. P. Kouwenhoven, D. van der Marel, and C. T. Foxon, Phys. Rev. Lett. **60**, 848 (1988).

[4] K. J. Thomas, J. T. Nicholls, M. Y. Simmons, M. Pepper, D. R. Mace, and D. A. Ritchie, Phys. Rev. Lett. **77**, 135 (1996).

[5] S. Tomonaga, Prog. Theor. Phys. **5**, 544 (1950).

[6] J. M. Luttinger, J. Math. Phys. **4**, 1154 (1963).

[7] L. I. Glazman, I. M. Ruzin, and B. I. Shklovskii, Phys. Rev. B **45**, 8454 (1992).

[8] F. Bloch, Z. Phys. **57**, 545 (1929).

[9] A. Gold and L. Calmels, Philos. Mag. Lett. **74**, 33 (1996).

[10] C. K. Wang and K.-F. Berggren, Phys. Rev. B **54**, 14 257 (1996).

[11] C. W. J. Beenakker and H. van Houten, in *Solid State Physics*, edited by H. Ehrenreich and D. Turnbull (Academic, New York, 1991).

[12] L. Martín-Moreno, J. T. Nicholls, N. K. Patel, and M. Pepper, J. Phys.: Condens. Matter **4**, 1323 (1992).

[13] H. van Houten, B. J. van Wees, J. E. Mooji, C. W. J. Beenakker, J. G. Williamson, and C. T. Foxon, Europhys. Lett. **5**, 721 (1988).

[14] N. K. Patel, J. T. Nicholls, L. Martín-Moreno, M. Pepper, J. E. F. Frost, D. A. Ritchie, and G. A. C. Jones, Phys. Rev. B **44**, 13 549 (1991).

[15] L. P. Kouwenhoven, B. J. van Wees, C. J. P. M. Harmans, J. G. Williamson, H. van Houten, C. W. J. Beenakker, C. T. Foxon,

and J. J. Harris, Phys. Rev. B **39**, 8040 (1989).
[16] K. F. Berggren, T. J. Thornton, D. J. Newson, and M. Pepper, Phys. Rev. Lett. **57**, 1769 (1986).
[17] K. J. Thomas, M. Y. Simmons, J. T. Nicholls, D. R. Mace, M. Pepper, and D. A. Ritchie, Appl. Phys. Lett. **67**, 109 (1995).
[18] N. K. Patel, J. T. Nicholls, L. Martín-Moreno, M. Pepper, J. E. F. Frost, D. A. Ritchie, and G. A. C. Jones, Phys. Rev. B **44**, 10 973 (1991).
[19] R. J. Stroh and M. Pepper, J. Phys.: Condens. Matter **1**, 8481 (1989).
[20] L. I. Glazman and A. I. Larkin, Semicond. Sci. Technol. **6**, 32 (1991).
[21] T. P. Smith III, J. A. Brum, J. M. Hong, C. M. Knoedler, H. Arnot, and L. Esaki, Phys. Rev. Lett. **61**, 585 (1988).
[22] Where there is a zero-field splitting Δ_i, we use the equation $eV_{sd}=2g_{\|}\mu_B B_{\|}S+\Delta_i$.
[23] A. M. White, I. Hinchliffe, P. J. Dean, and P. D. Greene, Solid State Commun. **10**, 497 (1972).
[24] B. J. van Wees, L. P. Kouwenhoven, E. M. M. Willems, C. J. P. M. Harmans, J. E. Mooij, H. van Houten, C. W. J. Beenakker, J. G. Williamson, and C. T. Foxon, Phys. Rev. B **43**, 12 431 (1991).
[25] A. Kristensen, P. E. Lindelof, J. B. Jensen, M. Zaffalon, J. Hollingbery, S. W. Pedersen, J. Nygard, H. Bruus, S. M. Reimann, C. B. Sorenson, M. Michel, and A. Forchel, Proceedings of the EP2DS Conference, Tokyo [Physica (to be published)].
[26] R. D. Tscheuschner and A. D. Wieck, Superlattices Microstruct. **20**, 615 (1996).
[27] P. Ramvall, N. Carlsson, I. Maximov, P. Omling, L. Samuelson, W. Seifert, Q. Wang, and S. Lourdudoss, Appl. Phys. Lett. **71**, 918 (1997).
[28] P. L. McEuen, B. W. Alphenaar, R. G. Wheeler, and R. N. Sacks, Surf. Sci. **229**, 312 (1990).
[29] J. H. Davies and J. A. Nixon, Phys. Rev. B **39**, 3423 (1989).
[30] J. T. Nicholls, J. E. F. Frost, M. Pepper, D. A. Ritchie, M. P. Grimshaw, and G. A. C. Jones, Phys. Rev. B **48**, 8866 (1993).
[31] A. Gold and A. Ghazali, Phys. Rev. B **41**, 8318 (1990).
[32] A. J. Daneshvar, C. J. B. Ford, A. R. Hamilton, M. Y. Simmons, M. Pepper, and D. A. Ritchie, Phys. Rev. B **55**, 13 409 (1997).
[33] L. I. Glazman and A. V. Khaetskii, J. Phys.: Condens. Matter **1**, 5005 (1989).
[34] G. Fasol and H. Sakaki, Jpn. J. Appl. Phys., Part 1 **33**, 879 (1994).
[35] C. K. Wang and K.-F. Berggren, Phys. Rev. B **57**, 4552 (1998).
[36] D. Schmeltzer, E. Kogan, R. Berkovits, and M. Kaveh, Philos. Mag. B **77**, 1189 (1998).
[37] C. L. Kane and M. P. A. Fisher, Phys. Rev. B **46**, 15 233 (1992).
[38] D. L. Maslov and M. Stone, Phys. Rev. B **52**, 5539 (1995).
[39] I. Safi and H. J. Schulz, Phys. Rev. B **52**, 17 040 (1995).
[40] V. V. Ponomarenko, Phys. Rev. B **52**, 8666 (1995).
[41] M. Ogata and H. Fukuyama, Phys. Rev. Lett. **732**, 468 (1994).
[42] D. L. Maslov, Phys. Rev. B **52**, 14 368 (1995).
[43] S. Tarucha, T. Honda, and T. Saku, Solid State Commun. **94**, 413 (1995).
[44] A. Yacoby, H. L. Stormer, N. S. Wingreen, L. N. Pfeiffer, K. W. Baldwin, and K. W. West, Phys. Rev. Lett. **77**, 4612 (1996).
[45] A. Y. Alekseev and V. V. Cheianov, Phys. Rev. B **57**, 6834 (1998).
[46] F. P. Milliken, C. P. Umbach, and R. A. Webb, Solid State Commun. **97**, 309 (1996).
[47] A. M. Chang, L. N. Pfeiffer, and K. W. West, Phys. Rev. Lett. **77**, 2538 (1996).